UNIVERSIDAD DE INVESTIGACIÓN DE TECNOLOGÍA EXPERIMENTAL YACHAY

Escuela de Ciencias Físicas y Nanotecnología

TÍTULO: Numerical Study of the Natural Inflation (NI) model

Trabajo de integración curricular presentado como requisito para la obtención del título de Físico

Autor:

Rony David Quinatoa Catucuago

Tutor:

Ph. D. Clara Inés Rojas Cely

Urcuquí, Julio 2023

AUTORÍA

Yo, **Quinatoa Catucuago Rony David**, con cédula de identidad 1050103991, declaro que las ideas, juicios, valoraciones, interpretaciones, consultas bibliográficas, definiciones y conceptualizaciones expuestas en el presente trabajo; así cómo, los procedimientos y herramientas utilizadas en la investigación, son de absoluta responsabilidad de el/la autora (a) del trabajo de integración curricular. Así mismo, me acojo a los reglamentos internos de la Universidad de Investigación de Tecnología Experimental Yachay.

Urcuquí, Julio 2023.

_____

Rony David Quinatoa Catucuago

CI: 1050103991

AUTORIZACIÓN DE PUBLICACIÓN

Yo, **Quinatoa Catucuago Rony David,** con cédula de identidad 1050103991, cedo a la Universidad de Investigación de Tecnología Experimental Yachay, los derechos de publicación de la presente obra, sin que deba haber un reconocimiento económico por este concepto. Declaro además que el texto del presente trabajo de titulación no podrá ser cedido a ninguna empresa editorial para su publicación u otros fines, sin contar previamente con la autorización escrita de la Universidad.

Asimismo, autorizo a la Universidad que realice la digitalización y publicación de este trabajo de integración curricular en el repositorio virtual, de conformidad a lo dispuesto en el Art. 144 de la Ley Orgánica de Educación Superior

Urcuquí, Julio 2023.

_____

Rony David Quinatoa Catucuago

CI: 1050103991

Abstract

The anisotropies of the cosmic microwave background (CMB) allow us to probe the primordial power spectrum generated in an epoch of cosmological inflation. We derive numerically the scalar and tensor power spectra in the Natural Inflation model (NI), which was originally proposed to solve the Big Bang problems such as the flatness problem, the horizon problem, and the CMB anisotropies. In this work, we perform a numerical study using the slow-roll approximation to the Friedmann equations to show the behavior of the Power Spectrum,P_S, and its value obtained with the observational data from the Planck Collaboration in the NI model which is $P_S \sim 3.51 \times 10^{-9}$, and compare it with the results obtained with this model $P_S \sim 2.0 \times 10^{-9}$ which is in good agreement with the observational results at 2σ confidence level.

Keywords: Inflation, power spectrum, Natural potential, scale factor, inflaton field.

Resumen

Las anisotropías del fondo cósmico de microondas (CMB) nos permiten sondear el espectro de energía primordial generado en una época de inflación cosmológica. Derivamos numéricamente los espectros de potencia escalar y tensorial en el modelo de Inflación Natural (NI), que se propuso originalmente para resolver los problemas del Big-Bang tales como el problema de planitud, el problema del horizonte y el las anisotropías del CMB. En este trabajo realizaremos un estudio numérico utilizando la aproximación de rodamiento lento a las ecuaciones de Friedmann, para mostrar el comportamiento del espectro de potencia, P_S, y su valor obtenido de los datos observacionales de la Colaboración Planck en el modelo Inflación Natural el cual $P_S \sim 3.51 \times 10^{-9}$, y compararlo con los resultados obtenidos con este modelo $P_S \sim 2.0 \times 10^{-9}$, el cual concuerda con los resultados observacionales a un nivel de confianza de 2σ.

Keywords: Inflación, espectro de potencia, potencial natural, factor de escala, campo de inflación.

Acknowledgements

First of all, I want to express my special thanks to my professor Clara Ines Rojas, who supported me all the way through this entire project.

I would like to thank my family for their interest and support all the time. My friends, at Yachay Tech University, for their help, encouragement, and all the happiest moments we ever had through our college life.

This is dedicated to the memory of my grandmother, wherever she is, I just hope she is looking after me...

Contents

List of Figures

Chapter 1

Introduction

Cosmic inflation is a model within the framework of theoretical physics (standard cosmological model) that explains the exponential expansion of the Universe at the beginning of time and solves some of the problems of the Standard Big Bang theory such as the horizon problem, the flatness problem, and CMB anisotropies[8]. For this purpose, inflation was first proposed by Alan Guth in 1981 as a mechanism to solve these problems. Guth used de Sitter's model that demonstrated the existence of a highly symmetric inflationary Universe, but it did not solve any cosmological problem mentioned before[8].

Furthermore, Guth proposed that as the early Universe cooled, it was trapped with high energy density in a false vacuum. This problem was solved with the model called "new inflation". According to this particular model, inflation took place due to a scalar field rolling down a potential energy hill, instead of the process of tunneling out of a false vacuum state[9]. Finally, Mukhanov demonstrated that the recently proposed inflationary model does not result in a completely symmetrical Universe[10]. Instead, it generates slight quantum fluctuations during the inflationary period. These minor fluctuations served as the fundamental precursors for all structures that were formed in the subsequent evolution of the Universe.

Natural Inflation (NI) indicates that there was a period of exponential expansion in the primal Universe. The expansion metric of the Universe increases exponentially. The expansion rate H (Hubble constant) is nearly constant, leading to high levels of symmetry and homogeneity[11][12]. These come from the observation of the Universe in the present, suggesting that it would have to have started from very "special" initial conditions (thermal and chemical equilibrium). Natural

1

Inflation solves these problems, as well as the flatness of its geometry, through the dynamics of a scalar field known as the inflaton[13].

In natural inflation, the sinusoidal function that describes the inflaton potential arises naturally from the symmetries of a hypothetical high-energy theory of particle physics. Thus, this potential allows the inflaton to slowly roll down its potential hill, driving to an exponential expansion of the Universe, where the duration and amplitude of this period can be simplified by fine-tuning the parameters of the potential in order to have consistency with the observational data obtained by the Collaborations Planck[14], COBE[15], and others.

Although Natural Inflation has been demonstrated to be a very good theory, because it can tackle the flatness problem in a simpler manner than other theories and due to its primary advantage which is the ability to generate primordial density perturbations consistent with cosmic microwave background (CMB) observations, to describe the period of exponential expansion, it remains a field of research in the scientific community (into the field of perturbation theory). However, it is commonly criticized for the lack of concrete connection to fundamental physics and the difficulty of producing the necessary symmetries in realistic particle physics scenarios. Nonetheless, Natural Inflation continues to inspire novel ideas and insights into the workings of the Universe, and its exploration remains a fruitful avenue for future research.

1.1   Problem Statement

The current explanation for the evolution of our Universe is the Hot Big Bang Theory. However, this theory has certain difficulties such as the flatness problem, the horizon problem, and the cosmic microwave anisotropies, among others[16][17]. In order for these problems to be overcome, a specific model of the inflation theory has been developed, the so-called Natural Inflation (NI). The most basic versions of this theory rely on a scalar field called ϕ, which gradually moves along a smooth potential function $V(\phi)$. Therefore, this thesis aims to address the issues of the Big Bang theory with the specific model of inflation in the slow-roll regime, and the study of the power spectrum P_S for this model.

1.2 General and Specific Objectives

1.2.1 General Objectives

Reproduce and study the power spectrum for the specific model of Natural Inflation, obtained with the result from the observation of the Planck satellite, into the slow-roll approximation.

1.2.2 Specific Objectives

1. Perform an analysis of the scale factor $a(t)$ in the slow-roll approximation and its time dependence.

Throughout this work natural units will be used ($c = \hbar = 1$) and reduced Planck mass $M_{Pl} = 1$.

Chapter 2

Methodology

2.1 The Big Bang

The foundation of modern cosmology is the Cosmological Principle, which posits that the Universe is uniform and homogeneous on a large scale[17][16]. This notion was first formulated mathematically by A. Einstein in his "General Theory of Relativity"[18][19], which explains the evolution of the Universe. Initially, this model hypothesized a static universe, but subsequent observations, such as those made by Hubble and colleagues, demonstrated its unpredictability (i.e., the expanding Universe). Furthermore, there is more observational evidence that together with the Hubble observations constitute the pillars supporting the Big Bang model: the existence of the Cosmic Microwave Background (CMB) and the abundance of light elements supported by the Big Bang Nucleosynthesis[6].

2.1.1 Basics of Cosmology theory

In a curved spacetime, the metric provides the measure of the physical distance between two points, based on a particular coordinate system that may be arbitrarily chosen.[20]. It is possible to use the most general metric from the Friedmann-Robertson-Walker (FRW) cosmology[20] due to the existence of a homogeneous and isotropic Universe for a large-scale distribution of galaxies and the uniformity of the CMB temperature

$$ds^2 = dt^2 - a(t)\left[\frac{dr^2}{1 - kr^2} + r^2(d\theta^2 + \sin^2\theta d\phi^2)\right], \tag{2.1}$$

where r, θ, ϕ are comoving spatial coordinates and t is the time. Here, the cosmic scale factor $a(t)$ is a time-dependent quantity that describes the expansion (nowadays a is taken to be 1). The quantity k represents the curvature of a three-dimensional space: k = 0 corresponds to a spatially flat, Euclidean universe, k > 0 to positive curvature (three-sphere), and k < 0 to negative curvature (saddle)[20].

It is useful to use the general form of Einstein's equations in the tensor form to describe appropriately the evolution of the Universe as

$$G_{\mu\nu} + \Lambda g_{\mu\nu} = 8\pi G T_{\mu\nu}, \tag{2.2}$$

here, it was used natural units, where $c = 1$. Also, G is the gravitational constant, Λ is the cosmological constant and $G_{\mu\nu}$ stands for the Einstein tensor which is given by

$$G_{\mu\nu} = R_{\mu\nu} - \frac{1}{2}g_{\mu\nu}R, \tag{2.3}$$

here $R_{\mu\nu}$ is the Ricci tensor and R is the Ricci scalar given by $R = g^{\mu\nu}R_{\mu\nu}$.

Friedmann equations are the key equations of cosmology[20], thus, applying the field equations of GR to the FRW metric we obtain

$$H^2 = \left(\frac{\dot{a}}{a}\right)^2 = \frac{8\pi G\rho}{3} - \frac{k}{a^2} + \frac{\Lambda}{3}, \tag{2.4}$$

and

$$\ddot{a} = -\frac{4\pi G}{p}(\rho + 3p) + \frac{\Lambda}{3}, \tag{2.5}$$

where $H = \frac{\dot{a}}{a}$ is the Hubble parameter, ρ is the total energy density of the Universe (the sum of matter, radiation, dark energy), and p is the total pressure of the universe (the sum of the pressures of each component). Equation 2.5 is also sometimes referred as the acceleration equation.

From the first law of thermodynamics ($dE = -pdV$), it is possible to derive the analog for the conservation of energy for each component (matter, radiation, dark energy) which is expressed as

$$d(a^3\rho_i) = p_i da^3, \tag{2.6}$$

the subscript i stands for matter, radiation, and dark energy. Thus, the evolution of the energy density is governed by the equation-of-state parameter[21]. In the case of a constant w_i

$$w_i = \frac{p_i}{\rho_i} = constant,, \tag{2.7}$$

where $\rho_i \propto (1 + z)^{3(1+w_i)}$.

Thus, the equation-of-state parameter for each component is

$$
\begin{aligned}
w_m &= 0, & \rho_m &\propto (1 + z)^3, & &\text{nonrelativistic matter,} \\
w_r &= \frac{1}{3}, & \rho_r &\propto (1 + z)^4, & &\text{radiation,} \\
w_{vac} &= -1, & \rho_{vac} &= \frac{\Lambda}{8\pi G}, & &\text{vacuum energy.}
\end{aligned}
\tag{2.8}
$$

For a flat Universe, the present energy density is given by

$$\rho_c = \frac{3H^2}{8\pi G}, \tag{2.9}$$

and its present value is $\rho_c = 8.10 \times 10^{-47} h^2$ GeV.

It is convenient to measure the energy density as a fraction of the critical density by defining the density parameter as

$$\Omega_i = \frac{\rho_i(t_0)}{\rho_c}, \tag{2.10}$$

$\Omega_0 > 1$ results in a positively curved Universe, while $\Omega_0 < 1$ gives a negatively curved Universe[22]. The information obtained from the CMB suggests that the Universe is nearly spatially flat ($\Omega = 1$).

Additionally, one can infer the evolution of the energy density with respect to the scale factor as follows

$$\rho \propto a^{-3(1+w)}, \tag{2.11}$$

then, we can get the relation for the different constituents[23][164]

$$
\begin{aligned}
\rho &\propto a^{-4}, & &\text{radiation,} \\
\rho &\propto a^{-3}, & &\text{matter,} \\
\rho &\propto a^0, & &\text{cosmological constant.}
\end{aligned}
\tag{2.12}
$$

Also, the evolution of the scale factor can be effectively described by its dependence on the dominant form of energy, as follows

$$a(t) \propto t^{\frac{2}{3}(1+w)},\tag{2.13}$$

for a constant w. Therefore, we have for the radiation-dominated era, given by $a(t) \propto t^{1/2}$; for the matter-dominated era, $a(t) \propto t^{2/3}$; and during the dark-energy dominated era, $a(t) \propto exp(Ht)$.

2.2   Evidences Big Bang Theory

2.2.1   Hubble law

About a century ago, a static Universe was the prevailing belief, and the idea of an evolving Universe was first proposed by Alexander Friedmann and Georges Lemaitre. Friedmann discovered in 1922 that Einstein's equations allowed for a dynamic Universe[24], while Lemaitre derived a non-static solution to Einstein's equations in 1927 and suggested that the Universe was expanding based on observational data[25]. Today, we have strong evidence to support the idea of an expanding Universe, and Hubble's law is one of the fundamental principles in modern cosmology that provides support for this expansion. Hubble's law, named after astronomer Edwin Hubble, was established in 1929 and provided conclusive evidence for the expansion of the Universe by showing a correlation between the recessional velocity and the distance of galaxies[26]. This law is also known as the Hubble-Lemaitre Law, and it is expressed as

$$v = H_0 d,\tag{2.14}$$

where v, d, and H_0 are the recessional velocity, the distance to the galaxy, and the Hubble constant at present time, respectively. This equation describes the linear relationship between the velocity and distance of galaxies and a constant rate of expansion given by H_0. Fig. 2.1 shows the Hubble diagram, which is the graphical representation of Hubble's Law, and it shows how the distances of the galaxies time ago were closer than nowadays.

The value H_0 denotes the unchanging rate of expansion in every direction, and it corresponds to the present value of the Hubble parameter, $H(t) = (1/a)(da/dt)$. The scale factor, a, is a variable that describes the Universe's expansion over time, and the Hubble parameter gauges the
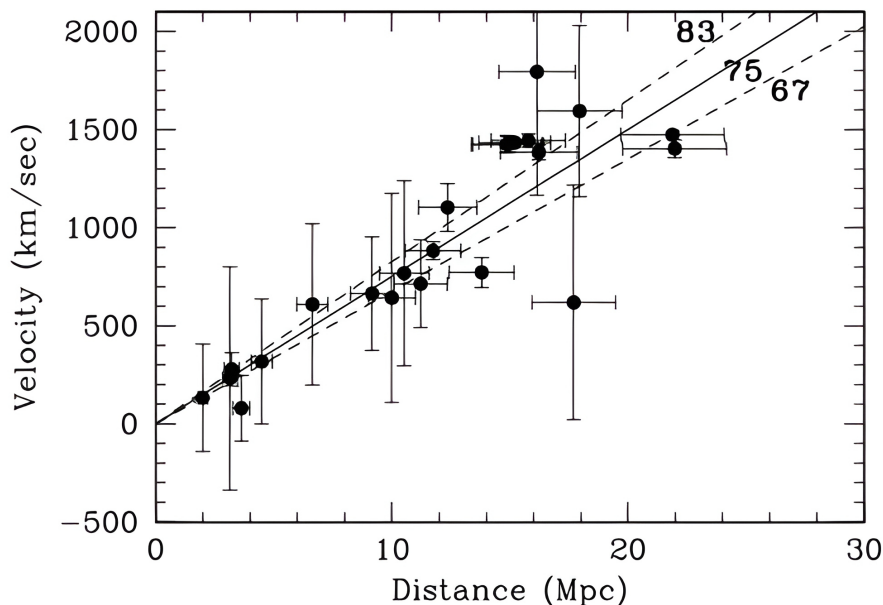
Figure 2.1: Hubble diagram from the Hubble Space Telescope Key project. Velocity vs. distance for galaxies with Cepheid distances[1]. The black dots represent the galaxies, and the error horizontal bars represent the measurements of the error in distance for type Ia supernovae with respect to the measurements of type II supernovae. The values for the Hubble constant H_0, are 67 kms^{-1}Mpc^{-1} for type Ia supernovae (dashed line) and 75 kms^{-1}Mpc^{-1} for type II supernovae (solid line).

rate of change in the scale factor. It is conventional to assign the value of $a = 1$ in the present day, and the Hubble Constant's value is parameterized by a dimensionless factor, h, as defined below

$$H_0 = 100h \, \text{km s}^{-1}\text{Mpc}^{-1}, \tag{2.15}$$

here Mpc is a unit called megaparsec and its value is 3.0856×10^{22}m. Ever since Hubble's measurement in 1929, the Hubble Constant's value has undergone changes, and currently, there is still a lack of agreement between observational measurements (Supernovae type Ia and CMB), on its precise value, with an uncertainty of 5%[27]. Researchers have used various methods and

observations to measure the value of the Hubble Constant, including analyzing Cepheids and supernovae[1 28 29], studying the cosmic microwave background radiation[30 16], examining the properties of accretion disks through H_2O masers[31 32], and observing quasars that are strongly lensed by galaxies[33]. Additionally, a combined analysis of both gravitational wave and electromagnetic data has also been utilized to determine H_0.

Currently, the value of H_0, often represented as h, is estimated to be around 0.7. This value has been derived from the analysis of multiple sources of data, which have helped to refine and improve our understanding of the Universe's expansion rate[34]. Despite this progress, there is still ongoing research and debate surrounding the exact value of the Hubble Constant, as different methods of measurement can lead to different results, as those reported for the Ia supernovae where the value of H_0 was found to be ranging from 54 ± 5 to 60 ± 6[35], and on the other hand, for the CMB observations, it was found through best-fit 67.32[14]. Nonetheless, scientists continue the efforts to refine our understanding of the Universe's expansion and help to further clarify the value of this important cosmological constant.

2.2.2   Big Bang Nucleosynthesis

The Big Bang theory is corroborated by three major historical proofs: the Universe's expansion, the cosmic microwave background, and primordial nucleosynthesis[36]. Big Bang nucleosynthesis (BBN) is the process that occurred in the first few minutes of the Universe's existence, where light elements (D,^{3}He, Li, and especially ^{4}He) were created through nuclear reactions. BBN is a crucial event in the history of the Universe as it laid the foundation for the formation of the first stars and galaxies.

During the early evolution of the Universe, before nucleosynthesis occurred, the Universe was at a high temperature and density. This allowed particles such as electrons, positrons, photons, neutrinos, nucleons, and heavier nuclei to be in chemical and thermal equilibrium due to high interaction rates[4] (weak, strong, and electromagnetic interactions).

BBN theory involves studying the weak and nuclear reactions in the context of a Universe that is expanding and cooling. In fact, it can be understood as the competition between the cosmic expansion rate and the particle reaction rates[2]. From the usual Friedmann equation, we can express the expansion rate as
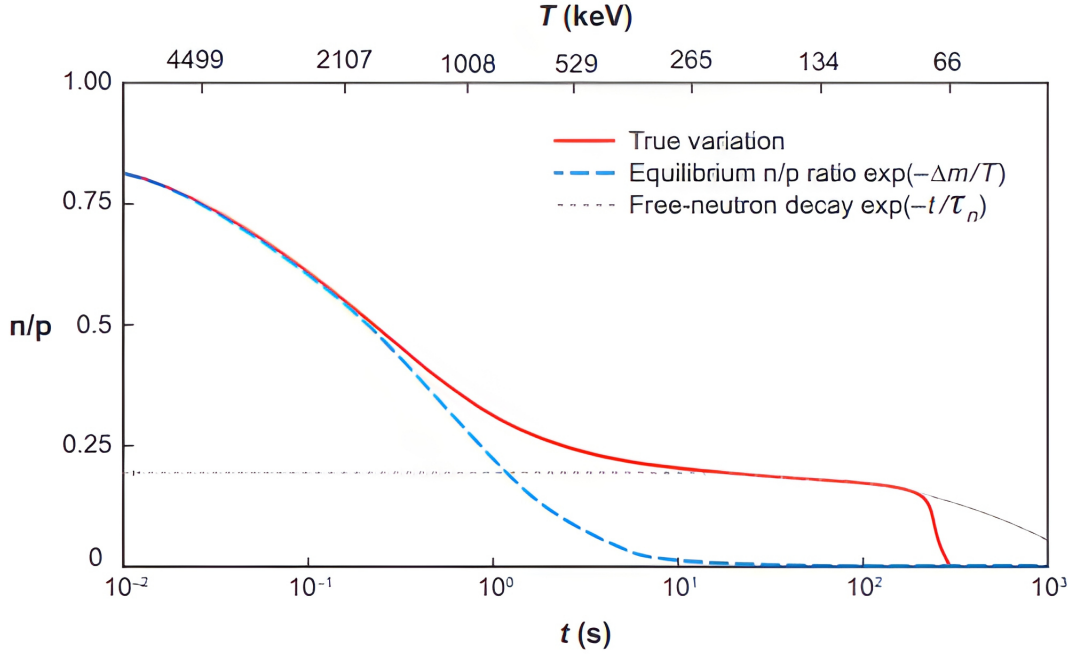
Figure 2.2: Time-temperature evolution of the neutron-proton ratio (n/p). The solid and dashed lines show the true and equilibrium variation of the n/p ratio, respectively. The dotted gray line indicates the free-neutron decay[2]

$$H^2 = \frac{8\pi G}{3}\rho \qquad \text{where,} \qquad H = \frac{\dot{a}}{a}, \tag{2.16}$$

where ρ is defined as the energy density, which in the early Universe was dominated by radiation (relativistic particles)

$$\rho_{rad} = \frac{\pi^2}{30}\left(2 + \frac{7}{2} + \frac{7}{4}N_\nu\right)T^4 = \frac{\pi^2}{30}g_*T^4. \tag{2.17}$$

where N_ν stands for the neutrino flavors which in the standard BBN $N_\nu = 3$. The production of light elements was sensitive to the physical conditions present during the early stages of the BBN at temperatures $T \leqslant 1$ MeV. Thus, above this temperature, weak interactions were in thermal equilibrium, particularly the processes[3]
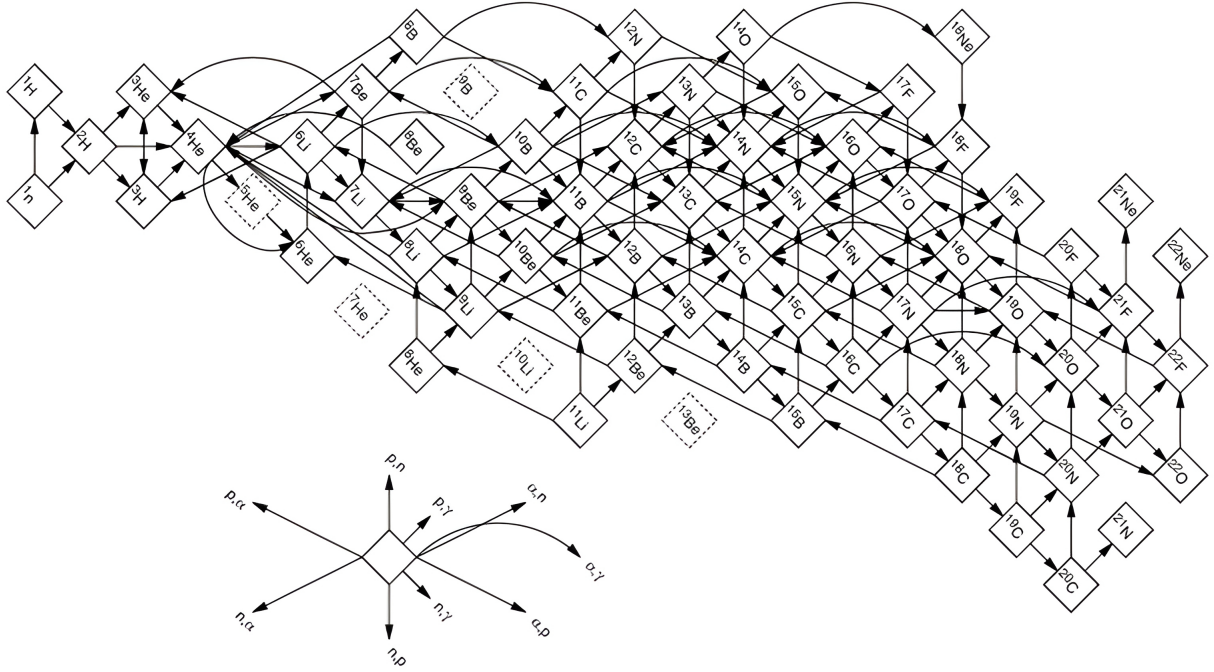
Figure 2.3: Nuclear network used for BBN calculations[3]. The BBN chain reaction goes from left, starting from the reaction of light elements (D, He); to the right, to form heavier elements (Li, C, B, etc.)

$$n + e^+ \longleftrightarrow p + \bar{\nu}_e,$$
$$n + \nu_e \longleftrightarrow p + e^-, \qquad\qquad (2.18)$$
$$n \longleftrightarrow p + e^- + \bar{\nu}_e,$$

where n, p, e^-, e^+, ν_e, and $\bar{\nu}_e$ stands for the neutron, proton, electron, positron, electron neutrino, and anti-electron neutrino particles, respectively; and these processes set the neutron to proton ratio fixed, so that $n/p = \exp^{-Q/T}$, where Q is the neutron-proton mass difference and it is equal to 1.293 MeV[32]. At temperatures greater than 1 MeV ($T \geqslant 1$ MeV), the neutron-proton ratio is almost the same ($n/p \simeq 1$). Then, as the temperature drop down, the neutron-proton rate fell faster than the Hubble expansion rate, resulting in the breaking of the chemical equilibrium at a

temperature $T_{fr} \simeq 0.8$ Mev, where the neutron fraction $n/p \simeq 1/6$. Then, the two-body reactions among neutrons, protons, $e^{\pm}$, and ν_e ($\bar{\nu}_e$) continue to influence the ratio of neutrons to protons causing it to continue decreasing, and leaving the neutrons to go free β-decay, until $n/p \simeq 1/7$. The variation of the n/p ratio is shown in Fig. 2.2 where n/p varies as T goes below 1 MeV.

The formation of deuterium, D (^{2}H), marks the beginning of the nucleosynthesis chain, such process is

$$n + p \longleftrightarrow D + \gamma, \tag{2.19}$$

at this stage, the photon temperature is below the deuterium binding energy $B_D = 2.2$ MeV. The deuterium production is delayed because of the high amount of photons per baryon, where the baryon-photon ratio is given by

$$\eta = \frac{n_b}{n_\gamma} \sim 10^{-9}. \tag{2.20}$$

Thus, when T drops well bellow B_D, the nuclear chain began, that is at $T = 0.1$ MeV[3]. Additionally, due to the relatively low density at this point, the only significant reactions are those involving 2-body. Fig.2.3 shows the beginning of the nuclear chain reaction to form light elements starting from D.

Once the BBN starts, neutrons and protons begin to combine to form heavier nucleons than D. Hence, in Fig.2.4 it is shown that the formation of helium started almost immediately after the formation of D, and then as time passes neutrons, protons, D and helium start to combine to form heavier elements like Lithium, Beryllium, and even Boron and Carbon. So now, it is easier to calculate the final density (n) of ^{4}He as it is very sensitive to the whole nuclear network, and consequently, we can express the mass fraction of the helium as the simple counting argument[43][2][37]

$$Y_p = \frac{2(n/p)}{1 + n/p} \simeq 0.25. \tag{2.21}$$

Since now each of these abundances can be measured, the BBN is one of the key cosmological tools used to test the Hot Big Bang model.
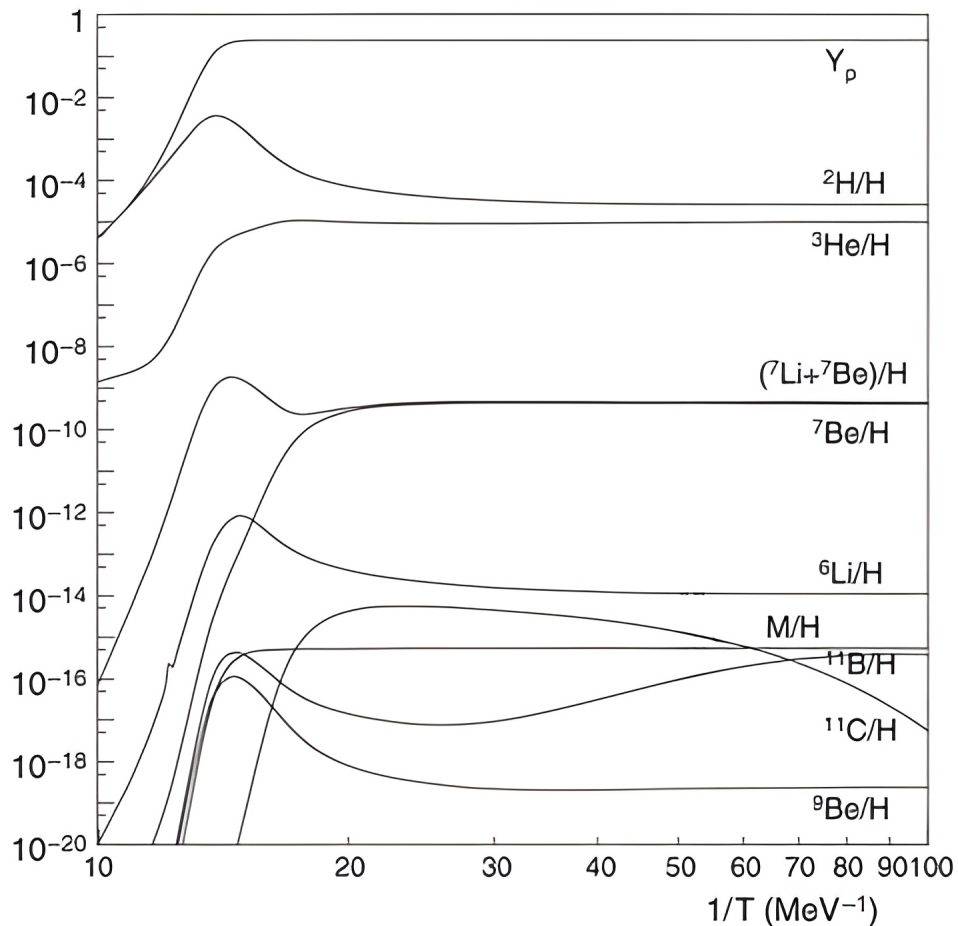
Figure 2.4: Time evolution of some nucleon abundances produced during the BBN[4]. The evolution of light nuclide abundances as a function of the temperature of the plasma starting from ^{2}H and H, until the formation of heavy nuclides C, B, etc.

2.2.3   Cosmic Microwave Background

The Big Bang theory is substantiated by a significant evidential element called the cosmic microwave background (CMB). When the temperature of the Universe was around 10^4 Kelvin, which corresponds to energies of approximately ~ 1 eV, free electrons and protons came together

to form neutral hydrogen atoms. Before this, any hydrogen formed was rapidly ionized by energetic photons present in the Universe. This epoch, which occurred at a redshift of $z = 1100$[6], marked the moment when the photons comprising the cosmic microwave background ceased interacting with any particles and started to travel freely through space. We can compute the number density of photons in the Universe at a redshift z which is given by

$$n_\gamma = 420(1 + z)^3 \text{cm}^{-3}, \tag{2.22}$$

where the factor $(1 + z)$ represents the linear scale at which the Universe has expanded since then. Additionally, the radiation temperature of the Universe is given by

$$T = T_0(1 + z), \tag{2.23}$$

where it is easy to observe how the conditions in the early stage of the Universe at high redshifts were hot and dense[38].

When looking back on them, we see the most powerful probes of the early Universe. Prior to recombination, the Universe was not transparent to electromagnetic radiation due to the scattering of photons by free electrons. However, as recombination took place, the density of free electrons decreased significantly, resulting in the separation of matter and radiation. This separation led to the Universe becoming transparent to light, allowing photons to travel freely without scattering[39].

In fact, just before the last scattering, the photon-baryon plasma was at thermal equilibrium, meaning that it should have a black-body spectrum. Then, we can calculate the intensity of a gas of photons for a black-body spectrum as

$$I_v = \frac{4\pi\hbar v^3/c^2}{\exp\left[2\pi\hbar v/k_B T\right] - 1}, \tag{2.24}$$

where v is the frequency, k_B is the Boltzmann constant and T is the temperature.

Fig. 2.5 shows the extraordinary agreement between the black body spectrum prediction of the Big Bang and the observations made by Far-InfraRed Absolute Spectrophotometer (FIRAS) instrument on the COBE satellite[5].

What is more important to remark is the fact that during 25 years of study, no anisotropies were detected in the CMB. This result conducted scientists to accept the view of a smooth Big Bang. However, later in 1992, the satellite mission COBE discovered anisotropies in the CMB,
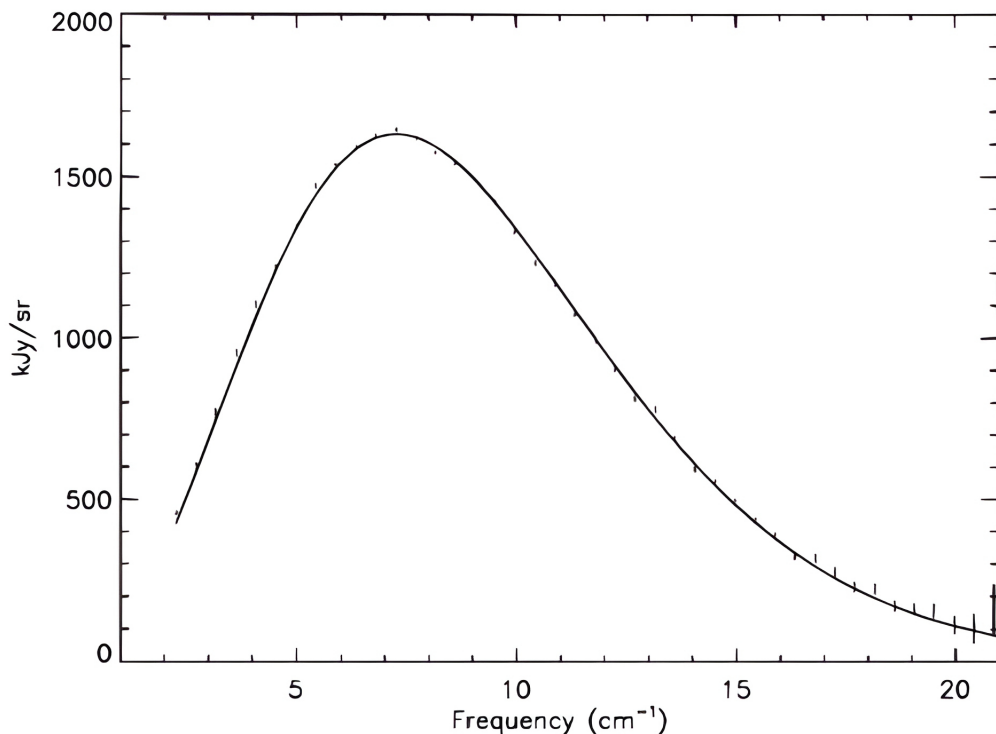
Figure 2.5: CMB spectrum from Far-Infrared Absolute Spectrophotometer (FIRAS) intrument of COBE satellite[5]. The plot shows a black-body spectrum with $T_0 = 2.728$ K.

changing the idea of a completely smooth early Universe. Small fluctuations in the temperature of the cosmic plasma were found(fractional temperature fluctuations) of the order 10^{-5}[6]. As a result, these fluctuations led to new studies focusing on new horizons such as the CMB polarization.

2.3   The Big Bang Theory Problems

2.3.1   The Horizon problem

The horizon problem is a fundamental issue in cosmology that emerges when trying to account for the consistent uniformity of cosmic microwave background radiation (CMB) noticed from opposing parts of the Universe. This problem can be expressed mathematically as follows: let θ

represent the angular size of a CMB region, and d represents the distance between two distinct points of the observable Universe. Then, the angle subtended by this distance at the observer is given by

$$\theta = \frac{d}{D}, \tag{2.25}$$

where D is the angular diameter distance to the point of observation. Assuming a flat Universe, D can be expressed as

$$D = a(t) \int_0^z \frac{dz'}{H(z')}, \tag{2.26}$$

where $a(t)$ is the scale factor, z is the redshift of the observed radiation, and $H(z)$ is the Hubble parameter at redshift z.

The cosmic microwave background (CMB) radiation can be traced back to the last scattering surface, which appeared at a redshift of roughly $z \sim 1100$. During this period, the Universe was considerably homogeneous, and temperature variations were roughly of the order of 10^{-5}[6]. Nevertheless, as light moves at a finite speed, sections of the Universe that were causally separated at the time of last scattering, i.e., separated by distances beyond the horizon distance, would not have had adequate time to reach thermal equilibrium before the radiation was released.

To understand this scenario, let us take a quick detour to consider the comoving distance η that light could have traveled since $t = 0$

$$\eta(t) = \int_0^t \frac{dt'}{a(t')}, \tag{2.27}$$

where we can quantify the extent of this problem by computing the comoving horizon η_* at recombination, which is the comoving distance light could have traveled from $\eta = 0$ to η_*. Then, for two different patches observed in the CMB, and under the assumption that at $t = 0$ there were only mater and radiation, we find that the comoving horizon at recombination is

$$\eta_* = \eta(a_*) \approx 281h^{-1}\text{Mpc}, \tag{2.28}$$

and, the comoving distance between patches on the CMB sky today separated by an angle θ, when θ is small, is defined as
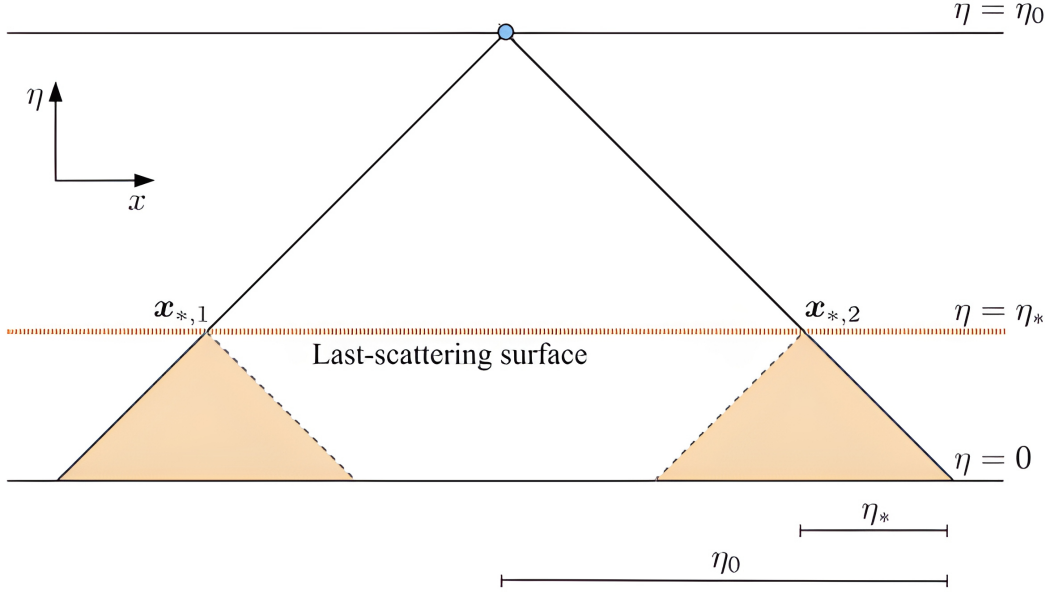
Figure 2.6: Illustration of the Horizon Problem in a η vs x diagram[6], where x is a coordinate, and for simplicity y and z were omitted. The observer detects the CMB signals coming from the past light cones, when these cones intersect the last-scattering surface (LSS) at $\eta = \eta_*$, where it is found to be uniform. Here, only the signals coming from the shaded areas below each point of contact in the LSS could have influenced the CMB photons emitted at $x_{*,1}$ and $x_{*,2}$. Since there is no overlapping between these 2 areas, there is no way for them to adjust to the same temperature if they started from different temperatures.

$$\chi(\theta) \simeq \chi_* \theta = (\eta_0 - \eta_*)\theta. \tag{2.29}$$

Now, $\eta_0 \approx 14200 h^{-1}$ Mpc, so that two patches in the CMB separated by

$$\theta \geq \frac{\eta_*}{\eta_0 - \eta_*} \approx 1.2°, \tag{2.30}$$

could not have been in thermal contact at recombination. From this, we can see that the factor between η_0 and η_* is on the order of 50 which is more strict than that in the diagram shown in

Fig. 2.6.

By rewriting Eq. 2.27 in terms of the $ln(a')$ we can see the problem from a different point of view, so

$$\eta(a) = \int_0^a dln(a')\frac{1}{a'H(a')},\qquad(2.31)$$

the comoving horizon η is now expressed in a logarithmic integral of the comoving Hubble radius, which is the distance that light can travel during one expansion time. It provides a criterion that tells us whether particles at that epoch can communicate with an e-fold (the measurement used to quantify the expansion or inflation of the universe) of expansion. Under the assumption that we made of the Universe at $t = 0$, where it is primarily controlled by either matter or radiation, the Hubble parameter H will scale in proportion to $a^{-3/2}$ or a^{-2}. This means that the comoving Hubble radius will continue to increase. As a result, the most recent epochs will significantly contribute to the value of η.

2.3.2 Flatness Problem

In order to have a better look at the flatness problem, we have to rewrite the Friedmann equation in terms of the density parameter Ω, ignoring the cosmological constant, as

$$\Omega_K \equiv -\frac{K}{a^2 H^2} = 1 - \Omega,\qquad(2.32)$$

where $\Omega = \frac{8\pi\rho}{3H^2}$. Then, we can get

$$\frac{d\Omega_K}{dlna} = (3w + 1)(1 - \Omega_K)\Omega_K,\qquad(2.33)$$

with $w = P/\rho$ being the equation of state parameter. Next, we can easy integrate it when $w = constant$, so

$$\frac{\Omega_{K0}}{\Omega_K(a)} = (1 - \Omega_{K0})\left(\frac{a}{a_0}\right)^{-1-3w} + \Omega_{K0}.\qquad(2.34)$$

Here, Ω_{K0} represents the curvature today. Since the observations[40] constrain it to $|\Omega - 1| \lesssim 0.01$, it implies that at radiation-matter equality and at a Planck time

$$|\Omega(a_{eq}) - 1| \lesssim 3 \times 10^{-6},$$
$$|\Omega(a_p) - 1| \lesssim 10^{-60}, \tag{2.35}$$

respectively. Thus, for a flat Universe $\Omega = 1$, it remains flat for all time; otherwise, the density parameter Ω evolves.

The flatness problem is simply that during the radiation and matter domination era, aH is decreasing with time, so that

$$|1 - \Omega| \propto t^{2/3},$$
$$|1 - \Omega| \propto t, \tag{2.36}$$

for matter-dominated and radiation-dominated eras, respectively. Ω_0 at the present time is not hugely different from 1, which implies that in the early time of the Universe, it had to be extremely close to 1[16]. Thus, to obtain our present Universe, it is necessary that certain conditions were met when the Universe was approximately 1s old, then

$$|\Omega(t_{nuc}) - 1| \lesssim 10^{-16}, \tag{2.37}$$

and, at prior times, Ω must be closer to 1.

The flatness problem states that the precise initial conditions required for a flat Universe are highly improbable. The majority of initial conditions result in either a closed Universe that collapses rapidly or an open Universe that enters a curvature-dominated phase[41][16] and rapidly cools to below 3K within the first second of its formation.

2.4 Inflation

The theory of inflation suggests that a phase in the Universe's history happened before the established Big Bang timeline. Observations of the products of Big Bang Nucleosynthesis (BBN)[42] indicate that the Universe was radiation-dominated between approximately $t \sim 1 - 100$ s after the Big Bang. These observations provide strong evidence that inflation must have occurred prior to this time period. During this period, inflation was supposedly governed by a type

of energy with $w \simeq -1$ or $H \simeq constant$. Therefore, by combining the Friedmann-Lemaître equations and assuming $K = 0$, one obtains the necessary conditions for inflation to take place.

The first condition is a decreasing comoving Hubble length with time (H^{-1}/a), which is given by the relation

$$\frac{d}{dt}\left(\frac{H^{-1}}{a}\right) < 0. \tag{2.38}$$

This result is fundamental in solving the horizon and flatness problems, and moreover, it is key for the mechanism to generate CMB fluctuations

The second condition, an accelerated expansion, where from Eq. 2.38, we have

$$\ddot{a} > 0. \tag{2.39}$$

And, the third condition, by which matter with a negative pressure is needed in order to have an accelerated expansion, so

$$\rho + 3p < 0 \qquad \text{or} \qquad p < -\frac{1}{3}\rho, \tag{2.40}$$

where p and ρ are the pressure and energy density, respectively.

We can measure the amount of expansion during inflation in terms of the number of e-folds [43], N, defined as

$$N(t) = \ln\left[\frac{a(t)}{a_i}\right], \tag{2.41}$$

where a_i stands for the scale factor at the beginning of inflation.

The motivation for the inflationary paradigm is strong because it offers a solution to all of the issues present in the standard cosmological model that have been previously mentioned.

2.4.1 Horizon problem solution

The conundrum of causally disconnected isothermal regions in the CMB observed at recombination can be explained naturally by inflation, provided that there was a significant number of e-folds of expansion. This is because a primordial phase of inflation would have caused even previously disconnected regions to become causally connected due to exponential expansion. Then, with the assumption of an exponential expansion during inflation

$$a(t) = a_i e^{H\Delta t}, \tag{2.42}$$

we can calculate the number of e-folds (N) needed to solve the horizon problem. The size of the current observable Universe d_{H_0} at the end of inflation, has to be smaller than the size of a causal region at the beginning of inflation d_{H_i}

$$d_{H_0}(t_0)\frac{a_{end}}{a_0} < d_{H_i}\frac{a_{end}}{a_i} = d_{H_i}(t_i)e^N, \tag{2.43}$$

where a_{end} represents the scale factor at the end of inflation. By assuming that inflation finishes at the Grand Unification scale ($\rho^{1/4} \sim 10^{16}$ GeV), then we need

$$N \sim \ln\left[\frac{T_0 d_{H_0}(t_0)}{T_{end} d_{H_i}(t_i)}\right] \gtrsim 57, \tag{2.44}$$

where T_0 is the temperature today, and where we have assumed $d_{H_i}(t_i) \sim l_{pl}T_{pl}/T_{end}$, where l_{pl} and T_{pl} are the Planck length and the Planck temperature, respectively. If the condition is met, the entire observable Universe originates from a single causal region prior to the initiation of inflation.

2.4.2 Flatness problem solution

Consider the curvature density

$$\Omega_K \equiv -\frac{K}{a^2 H^2} = 1 - \Omega, \tag{2.45}$$

in order for Ω_K to decrease, there must be an epoch in which $1/aH$ decreases with time, which means that we got to have an accelerated expansion

$$\frac{d}{dt}\left(\frac{H^{-1}}{a}\right) < 0 \qquad \rightarrow \qquad \ddot{a} > 0, \tag{2.46}$$

as we saw before, if the comoving Hubble length decreases with time, the Universe is driven toward flatness. Along with the exponential growth of inflation, we get

$$|\Omega - 1| \propto e^{-2Ht}, \tag{2.47}$$

where it is clear that in time $|\Omega - 1|$ tends to 0 exponentially. This enables a Universe that is exceedingly flat. In fact, if we make the assumption of $H \simeq 1$ during inflation, we have

$$|\Omega_K(a_{end})| = |\Omega_K(a_i)|e^{-2N}, \tag{2.48}$$

and additionally, with $N \gtrsim 70$ and a curvature of the order of unity at the Planck scale, this conducts the flatness problem to solve itself naturally.

2.5 Physics of inflation

2.5.1 Scalar fields

The most basic model that can lead to a period of inflation involves a sole scalar field called ϕ, which is referred to as the inflaton.

The scalar field plus gravity has the following action[44][43]

$$S = \int d^4x \sqrt{-g} \left[\frac{M_{Pl}^2}{2}R + \frac{1}{2}g^{\mu\nu}\partial_\mu\phi\partial_\nu\phi - V(\phi) \right] = S_{EH} + S_\phi, \tag{2.49}$$

here, M_{pl} is the reduced Planck mass. Also, the first term corresponds to the Einstein-Hilbert term present in General Relativity (GR). The second and third terms depict the effect of a scalar field S_ϕ. The potential function, $V(\phi)$ describes the scalar field's self-interactions. For us to know what happens, we need to take a look at the evolution of space-time, so we need the scalar field stress tensor, given by

$$T_{\mu\nu}^{(\phi)} = -\frac{2}{\sqrt{-g}}\frac{\delta S_\phi}{\delta g^{\mu\nu}} = \partial_\mu\phi\partial_\nu\phi - g_{\mu\nu}\left(\frac{1}{2}\partial_\rho\phi\partial^\rho\phi + V(\phi)\right), \tag{2.50}$$

and the scalar field's equation of motion

$$\frac{\delta S}{\delta \phi} = \frac{1}{\sqrt{-g}}\partial_\mu(\sqrt{-g}\partial^\mu\phi) + V'_\phi = 0. \tag{2.51}$$

Assuming the FRW metric from Eq. 2.1, and for a homogeneous field configuration, we can obtain the energy density and pressure, as

$$\rho_\phi = \frac{1}{2}\dot{\phi}^2 + V(\phi), \tag{2.52}$$

$$p_\phi = \frac{1}{2}\dot{\phi}^2 - V(\phi). \tag{2.53}$$

Consequently, the equation of state is

$$w_\phi = \frac{p_\phi}{\rho_\phi} = \frac{\frac{1}{2}\dot{\phi}^2 - V(\phi)}{\frac{1}{2}\dot{\phi}^2 + V(\phi)}. \tag{2.54}$$

Thus, if the potential energy dominates over the kinetic energy, this leads to negative pressure,

$$\dot{\phi}^2 \ll V(\phi) \qquad \Rightarrow \qquad w_\phi \simeq -1 < -\frac{1}{3}, \tag{2.55}$$

and consequently to an accelerated expansion, as reported by the Supernova Cosmology Project[45] and the High-z Supernova Search Team[46] back in 1998. Then, equations of motion for the dynamics of the scalar field are obtained

$$\ddot{\phi} + 3H\dot{\phi} = -\frac{dV}{d\phi}, \qquad \text{and} \qquad H^2 = \frac{1}{3}\left[\frac{1}{2}\dot{\phi}^2 + V(\phi)\right]. \tag{2.56}$$

The equation of motion for this is equivalent to that of a particle moving along its potential and rolling downwards, where this particle is subjected to friction though the $H\dot{\phi}$ term.

2.5.2 Slow-roll inflation

In order for inflation to be highly effective, the potential in the equations (2.56) must greatly outweigh the kinetic terms. The slow-roll approximation involves disregarding the kinetic terms and the field's second-order time derivatives, such that

$$\dot{\phi}^2 \ll V(\phi), \qquad \qquad \ddot{\Phi} \ll 3H\dot{\phi}, \tag{2.57}$$

this means that

$$\epsilon = \epsilon_H = -\frac{\dot{H}}{H^2} \sim \frac{\dot{\phi}^2}{V} \ll 1, \tag{2.58}$$

which is known as a slow-roll parameter, and it is related to the evolution of the Hubble parameter. In order to have sustained accelerated expansion, $\ddot{\phi}$ has to be very small, so that

$$|\ddot{\phi}| \ll |3H\dot{\phi}|, |V'(\phi)|, \tag{2.59}$$

and this requires the second slow-roll parameter to be small

$$\eta = -\frac{\ddot{\phi}}{H\dot{\phi}} = \epsilon - \frac{1}{2}\frac{d\epsilon}{dN}, \tag{2.60}$$

where $|\eta| < 1$ ensures a small change of ϵ per e-fold.

Another way to express the slow-roll parameters is related to the potential, as follows

$$\epsilon_V = \frac{M_{Pl}^2}{2}\left(\frac{V'}{V}\right)^2, \tag{2.61}$$

and

$$\eta_V = M_{Pl}^2\left(\frac{V''}{V}\right). \tag{2.62}$$

In the slow-roll regime.

$$\epsilon_V \ll 1, \qquad \text{and} \qquad |\eta| \ll 1, \tag{2.63}$$

and the background evolution can be expressed as

$$H^2 \simeq \frac{V(\phi)}{3M_{Pl}}, \tag{2.64}$$

$$3H\dot{\phi} \simeq -V'(\phi). \tag{2.65}$$

The number of e-foldings N is commonly used to measure the amount of inflation that has occurred, and it is expressed as:

$$N(t) = \ln\left[\frac{a(t_{end})}{a(t)}\right], \tag{2.66}$$

where t_{end} is the time at the end of inflation. Also, this can be written in terms of the potential in the following way

$$N = \int_t^{t_{end}} H dt \simeq \frac{1}{M_{Pl}}\int_{\phi_{end}}^{\phi}\frac{V}{V'}d\phi, \tag{2.67}$$

and in terms of the scalar potential

$$N = \int_{\phi_{end}}^{\phi} \frac{d\phi}{\sqrt{2\epsilon}} \approx \int_{\phi_{end}}^{\phi} \frac{d\phi}{\sqrt{2\epsilon_V}}, \tag{2.68}$$

where the values of ϕ_{end} are determined by the condition $\epsilon(\phi_{end}) = 1$ if inflation ends due to violation of the slow-roll condition [16]. Additionally, the number of e-folds of inflation required to resolve the flatness and horizon problem is approximately 60.

2.6 Power Spectrum of Natural Inflation Model

2.6.1 The power spectrum in terms of tensor and scalar spectral index

The power spectrum is an important instrument for describing the attributes of the fluctuations of the inflationary field. The spectra of scalar and tensor perturbations that originated in the early Universe are expressed in terms of a pivot scale of k [47][30] (the wavenumber (scale) at which the amplitude, A, is measured), denoted by k_*. These spectra are defined by

$$\mathcal{P}_{\mathcal{R}}(k) = A_s \left(\frac{k}{k_*}\right)^{n_s - 1 + \frac{1}{2}\frac{dn_s}{d\ln k}\ln\left(\frac{k}{k_*}\right) + \frac{1}{6}\frac{d^2 n_s}{d\ln k^2}\left(\ln\left(\frac{k}{k_*}\right)\right)^2 + ...}, \tag{2.69}$$

$$\mathcal{P}_t(k) = A_t \left(\frac{k}{k_*}\right)^{n_t + \frac{1}{2}\frac{dn_t}{d\ln k}\ln\left(\frac{k}{k_*}\right) + ...}, \tag{2.70}$$

where A_s and A_t are the scalar and tensor amplitude, respectively. n_s, n_t, $dn_s/d\ln k$, $dn_t/d\ln k$, and $d^2 n_s/d\ln k^2$ are the scalar and tensor spectral indices, and the running of the scalar and tensor spectral indices, respectively. Additionally, with the 2 spectral indices defined, the tensor-to-scalar ratio can be expressed as [47]

$$r = \frac{\mathcal{P}_t(k_*)}{\mathcal{P}_{\mathcal{R}(k_*)}}. \tag{2.71}$$

For the slow-roll regime, Eq. 2.69 and Eq. 2.6.1 can be expressed, for the single field model [48], as

$$\mathcal{P}_{\mathcal{R}}(k) \simeq \frac{2}{3\pi M_{Pl}^6} \frac{V^3}{V'^2}, \tag{2.72}$$

and

$$\mathcal{P}_t(k) \simeq \frac{16V}{3\pi M_{Pl}^4}, \tag{2.73}$$

under the consideration of the power spectra up to the lowest powers of the slow-roll parameters[48].
On the other hand, by using the relation

$$\frac{d}{dlnk} \simeq -M_{Pl}^2 \frac{V'}{V} \frac{d}{d\phi}, \tag{2.74}$$

we can obtain the scalar and tensor spectral indices and their corresponding running terms in
terms of the slow-roll parameters up to the first-order in the slow-roll parameters, ϵ_V and η_V, as

$$n_s(k) \simeq 1 - 6\epsilon_V + 2\eta_V, \tag{2.75}$$

$$\frac{dn_s}{dlnk} \simeq 16\eta_V\epsilon_V - 24\epsilon_V^2 - 2\xi_V^2, \tag{2.76}$$

$$\frac{d^2n_s(k)}{dlnk^2} \simeq 192\epsilon_V^3 - 192\epsilon_V^2\eta_V + 32\epsilon_V\eta_V^2 + 24\epsilon_V\xi_V^2 - 2\eta_V\xi_V^2 - 2\varpi_V^3, \tag{2.77}$$

and

$$n_t(k) \simeq -2\epsilon_V, \tag{2.78}$$

$$\frac{dn_t(k)}{dlnk} \simeq 4\epsilon_V\eta_V - 8\epsilon_V^2, \tag{2.79}$$

stands for the scalar and tensor perturbations, respectively, where

$$\xi_V^2 = M_{Pl}^4 \frac{V'V'''}{V^2}, \qquad \text{and} \qquad \varpi_V^3 = M_{Pl}^6 \frac{V'^2V''''}{V^3}. \tag{2.80}$$

Finally, the tensor-to-scalar ratio in terms of the slow-roll parameters is given by

$$r = \frac{\mathcal{P}_t(k_*)}{\mathcal{P}_{\mathcal{R}(k_*)}} \simeq 16\epsilon_V \simeq -8n_t. \tag{2.81}$$

2.6.2   Power Spectrum for the Natural Inflation Model

Natural inflation is one of the best scenarios to show the inflationary expansion in the early Universe [12]. The single field potential is sufficiently flat, and it is guaranteed by a shift symmetry that is perturbatively exact, where its flatness can only be broken by non-perturbative effects (i.e. instanton effects, string theory corrections). Inflationary potential presents "wiggles" (caused when instead of a pure cosine-potential we thus expect a more complicated picture including higher harmonics as subleading instanton effects [7]) that change the predictions with respect to the CMB observations in which in comparison with the power-law model, the scalar power spectrum principally deviates from it. [7]
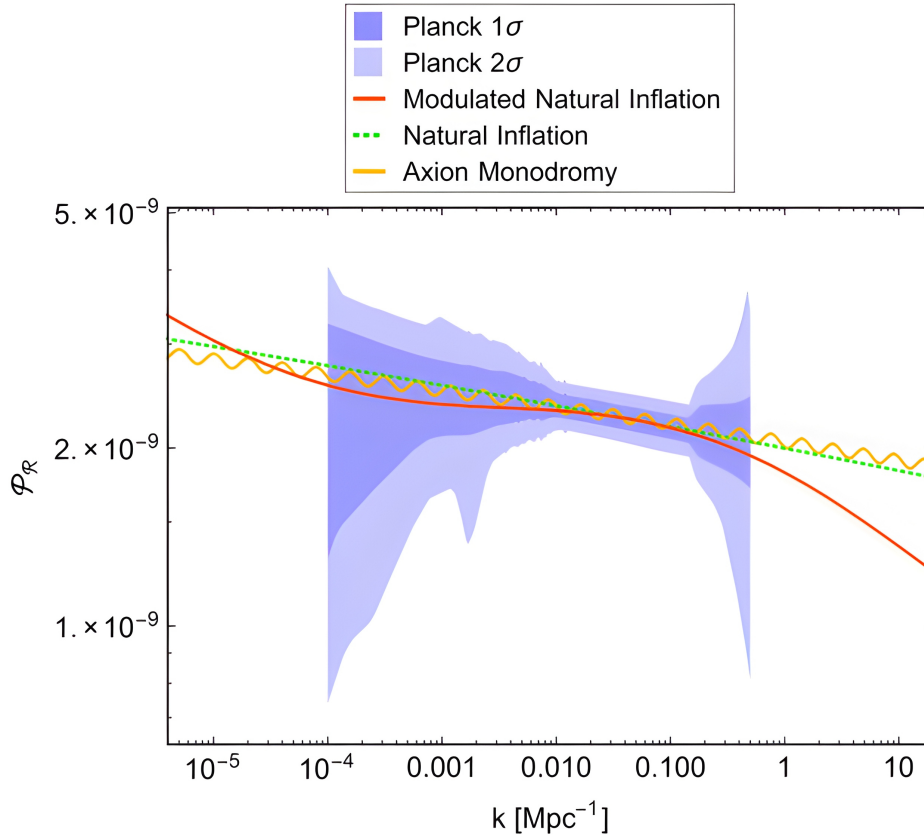

Figure 2.7: Power Spectra of the Natural Inflation model (green line), and for a Modulated Natural Inflation model (red line), compared to the Planck reconstructed power spectrum [7]

The distribution of density perturbations generated during the inflationary period (scalar power spectrum) describes the amplitude of these perturbations as a function of their wavelength[49], and it is usually represented as a plot of the amplitude logarithm versus the wavelength logarithm.

In natural inflation, the scalar power spectrum is a key quantity that can be used to describe the model. Specifically, natural inflation predicts a certain shape for the scalar power spectrum, which differs from other inflationary models as shown in Fig. 2.7[49], where we compare the pure natural inflation power spectrum with a slightly different modulated natural inflation model (modulated potential by instantons), which gives rise to a different behavior for the power spectrum. Thus, showing that the exponential expansion in the early stages of inflation depends on the model of inflation used.
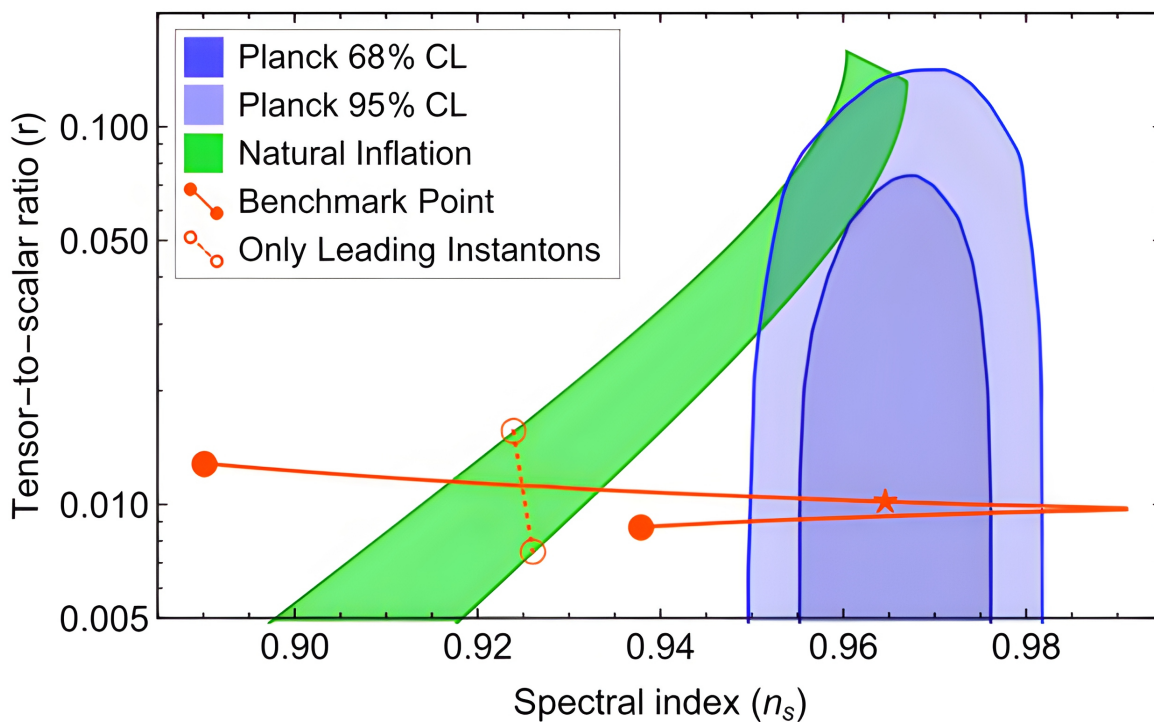
Figure 2.8: Tensor-to-scalar ratio vs spectral index (r vs n_s), assuming $N_* = 50 - 60$. Natural potential band and the most recent Planck results[7].

Another quantity useful to characterize the inflation of the Universe is the tensor-to-scalar

ratio r. This provides important information about the physics of the inflationary epoch and the nature of the gravitational waves produced during this epoch[7].

For Natural Inflation, this quantity is given by[11]

$$r = \frac{8}{N} \sin^2\left(\frac{N\phi}{f}\right),$$
(2.82)

where ϕ is the inflaton field, f is the symmetry breaking scale, and N is the number of e-folds of inflation. Fig. 2.8 shows the behavior of the tensor-to-scalar ratio for the natural inflation model, which is in good agreement with the results from the Planck data at 95% confidence level[7].

Chapter 3

Results & Discussion

3.1 Natural Inflation

3.1.1 Natural Inflation Potential

The paradigm that the early Universe underwent a phase of single-field slow-roll inflation is increasingly supported by accurate measurements of the CMB radiation[50]. In this case, Natural inflation was first proposed by Freese, Frieman, and Olinto[12] in 1990 in order to solve the so-called fine-tuning problem of inflationary models. Specifically, the inflaton potential $V(\phi)$ must possess enough flatness to produce the necessary inflation and ensure the appropriate normalization for the anisotropies found by observations in the cosmic microwave background. Natural inflation uses a symmetry-breaking mechanism to generate a periodic potential with numerous hills and valleys, thereby enabling sufficient inflation to occur. The resulting inflaton potential generates a distinct signature in the cosmic microwave background radiation, which can be observed and analyzed by scientists.

The potential used to provide such information has the form

$$V(\phi) = M^4 \left[1 + \cos\left(\frac{\phi}{f}\right) \right],$$ (3.1)

here, M represents the mass that is obtained from the CMB normalization[17], Eq. (3.9), and f is obtained from the observational results[14], and its value is $f = 5.5$ (dimensionless). V_ϕ is
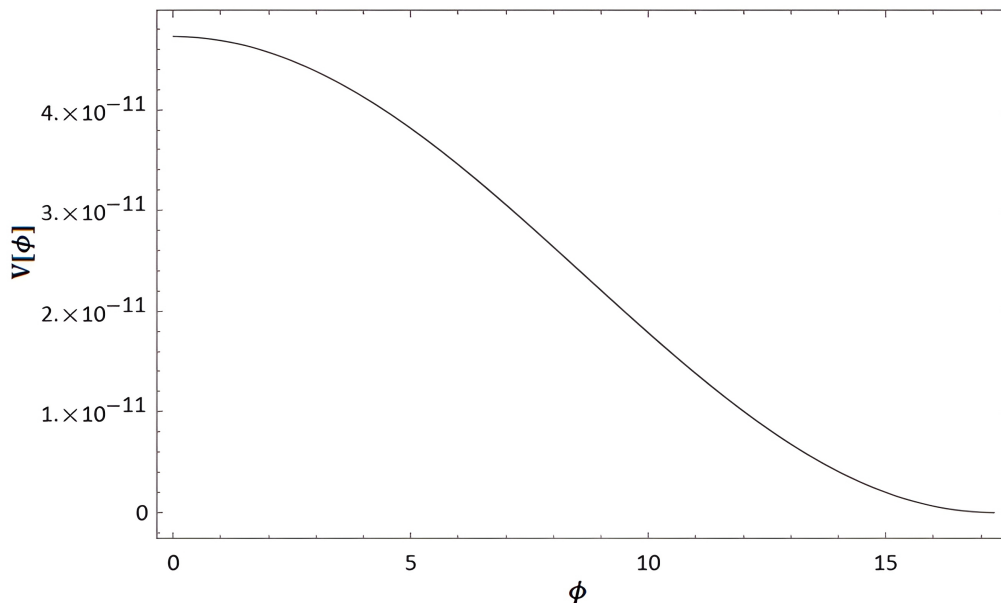
Figure 3.1: Natural Inflation potential V (Eq. 3.1) as a function of the scalar field ϕ. All variables are expressed in Planck units.

also called inflaton potential, which makes use of the Pseudo Nambu-Goldston boson particle where its flatness is ensured thanks to shifting symmetries[51]. This model has been successful in describing the features of CMB radiation such as the amplitude and the spectral index of density fluctuations.

In Fig. 3.1 it is easy to see that inflation at the very beginning depends only on the potential energy which slowly decreases as inflation proceeds in time, showing the shape of a hill.

3.1.2   Inflaton Field ϕ

In natural inflation, the sinusoidal shape of the potential is similar to the potential of a simple harmonic oscillator, where the inflaton scalar field slowly rolls down the potential energy hill towards the minimum of the potential which is located at the end of the inflation. This is the field that drives the amount of inflation and the direction in which the expansion proceeds. In particular, for natural inflation, the slow rolling of the inflaton field is achieved by fine-tuning the
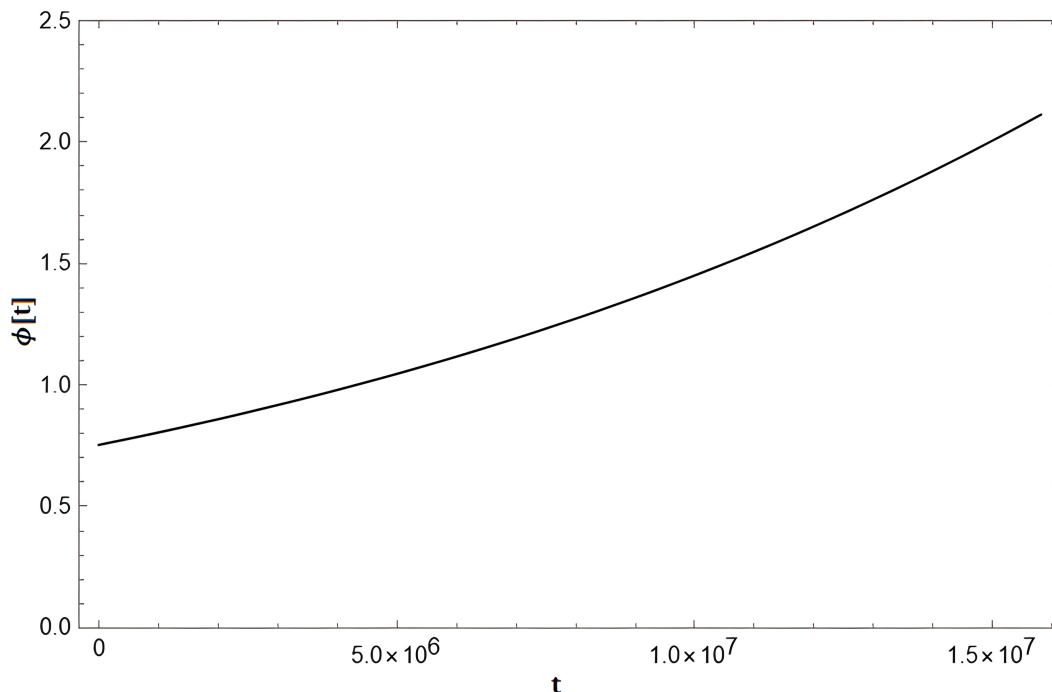
Figure 3.2: Behavior of the scalar field ϕ as a function of time in the slow-roll regime obtained in Eq. (3.12). Variables are expressed in Planck units.

slope of the sinusoidal potential.

The inflaton scalar field ϕ is obtained from the equations of motion, Eq. (2.64) and Eq. (2.65), stated in Chapter 2, where its behavior depends on the model of inflation used. As a result, for the slow-roll approximation, the prediction of the behavior obtained for the scalar field is the almost same as for the general regime solving the complete Friedmann equations, with some differences at the end of the inflation.

In the slow-roll regime, the behavior of the inflaton scalar field at the end of the inflation presents inconsistencies because it does not take into account the complete solution of the Friedmann equations, it neglects the kinetic term which in the complete Friedmann equations give rise to oscillations at the end of the inflation. This causes a problem when trying to describe properly the last *e*-folds of the natural inflation model, leading the model to be ineffective when trying to analyze the end of inflation.

3.1.3   Scale factor of inflation $a(t)$ in the slow-roll regime

As seen before, the scale factor is intimately related to the Hubble parameter, which controls the rate at which the Universe expands[16]. For natural inflation, the Hubble parameter is almost constant, which means that the scale factor increases exponentially with time as $a \propto e^{Ht}$, as shown in Fig. 3.3.
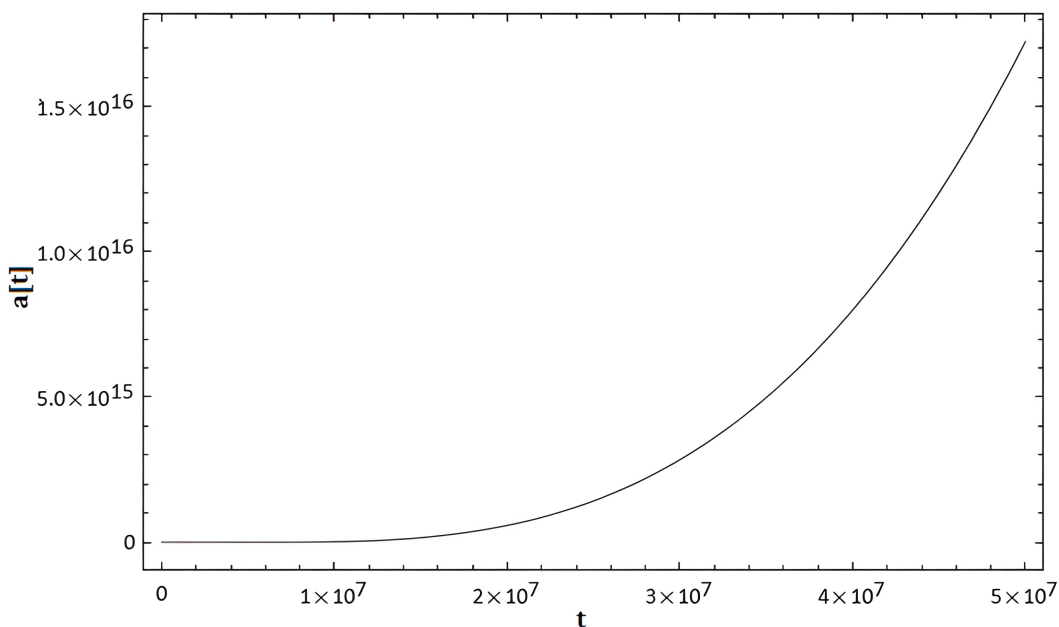
Figure 3.3: Exponential behavior of the scale factor $a(t)$ obtained in Eq. (3.14) as a function of time. Variables are expressed in Planck units.

This exponential growth is responsible for solving some of the problems presented in the Standard Big Bang Theory, principally the horizon problem.

Furthermore, the scale factor also establishes a significant relation with the spectral index n_s, described by Eq. (2.75), and the tensor-to-scalar ratio described by Eq. 2.81, which describes the dependence of the power spectrum on the scale factor. As the scale factor increases exponentially with time during inflation, quantum fluctuations scale to cosmological proportions. These fluctuations give rise to density perturbations which affect the value of r, where particularly for natural

inflation is $\ll 1$, which is in agreement with the results obtained by Planck at 95% confidence level[7].

3.1.4   Power Spectrum of Natural Inflation in the Slow-roll Regime

In the slow roll regime, for this model of Natural Inflation, the order of the power spectrum is of 10^{-9}, where it coincides with the results obtained with Planck satellite at 2σ confidence level[7]. Moreover, this is also shown in Fig. 2.7 where the pure natural inflation model (solved with the complete Friedmann equation) compared to the slow-roll approximation differs by a few units, $P_S \sim 3.5 \times 10^{-9}$ for the Planck Collaboration results and $P_S \sim 2.0 \times 10^{-9}$ for the slow-roll approximation results reported in this work, but it shows the same behavior and the same shape, meaning that our approximation matches the real almost perfectly the real results.
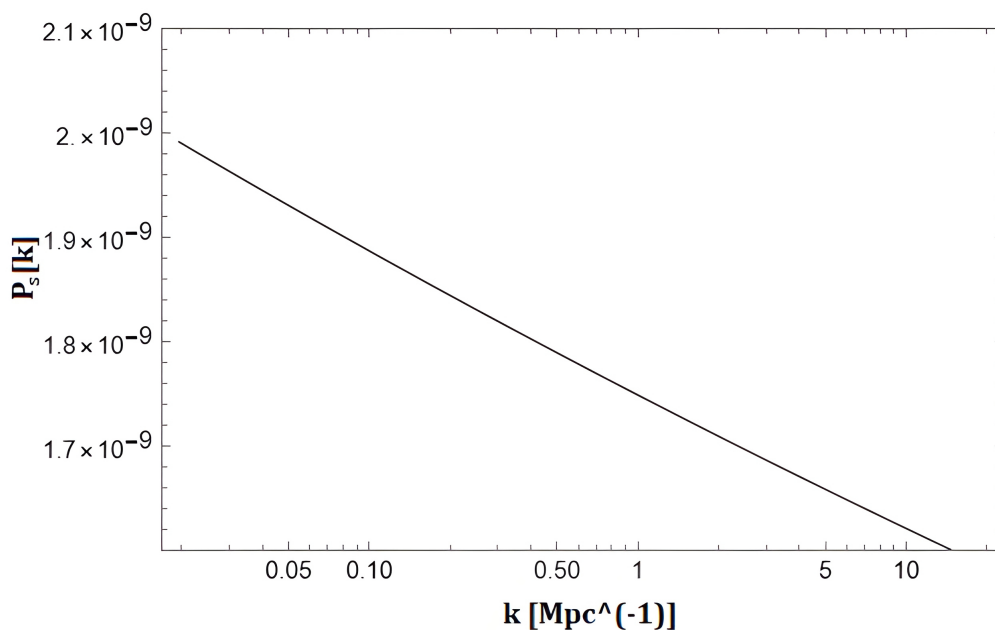

Figure 3.4: Log plot of the Power Spectrum P_S for the Natural Potential $V(\phi)$, in the slow-roll regime

The Planck data[14][30] (Fig. 2.7) shows that the amplitude of the scalar power spectrum is

consistent with the predictions of the Natural Inflation Model, with an energy scale of inflation of $\Lambda = (7.8 \pm +6935780.5) \times 10^{15}$ GeV [14][52]. These results differ from other models like the chaotic inflationary model, Large Field, etc, which give values completely different from those for Natural Inflation. Moreover, the shape of the power spectrum changes significantly with a small perturbation to the model as shown in Fig. 2.7.

3.2   Slow-Roll Analysis

By using the natural potential (Eq. (3.1)), and the equations of slow-roll parameters (Eq. (2.61) and Eq. (2.62)) the solution for the slow-roll parameters are given by

$$\epsilon = \frac{1}{2f^2} \frac{\sin^2\left(\frac{\phi}{f}\right)}{\left(1 + \cos\left(\frac{\phi}{f}\right)\right)^2},\tag{3.2}$$

and

$$\eta = -\frac{1}{f^2} - \frac{\cos\left(\frac{\phi}{f}\right)}{1 + \cos\left(\frac{\phi}{f}\right)},\tag{3.3}$$

where we have used for this calculations $M_{Pl} = 1$. These are all increasing functions that depends on the field, ϕ. Thus, it is easy to see that they evolve increasingly during inflation. By the fact that at the end of inflation $\epsilon = 1$

$$\epsilon = \frac{1}{2f} \frac{\sin^2\left(\frac{\phi}{f}\right)}{(1 + \cos\left(\frac{\phi}{f}\right))^2} = 1,\tag{3.4}$$

then, we can get the expression for ϕ at the end of the inflation as

$$\phi_{end} = f \arccos\left(\frac{1 - 2f^2}{1 + 2f^2}\right).\tag{3.5}$$

Now, we can easily compute the number of e-foldings which has the following form

$$N = f^2 \ln\left(\frac{1 - \cos\left(\frac{\phi_{end}}{f}\right)}{1 - \cos\left(\frac{\phi}{f}\right)}\right).\tag{3.6}$$

In order to calculate the scalar potential of the natural inflation, by observational evidence, it is suggested that the number of *e*-foldings N at the end of inflation has to be $N \sim 50 - 60$. Thus now, we compute the equations of motion, Eq. (2.64) and Eq. (2.65), in the slow-roll regime as follows

$$H^2 = \frac{M^4}{3}\left[1 + \cos\left(\frac{\phi}{f}\right)\right], \tag{3.7}$$

$$H = \frac{M^2}{\sqrt{3}}\left[1 + \cos\left(\frac{\phi}{f}\right)\right]^{1/2}, \tag{3.8}$$

where M is obtained from CMB normalization [17] as

$$M^4 = \frac{12 P_s \pi^2 \sin^2(\phi/f)}{f^2[1 + \cos(\phi/f)]^3} \tag{3.9}$$

and

$$3H\dot{\phi} = \frac{M^4}{f}\sin\left(\frac{\phi}{f}\right), \tag{3.10}$$

then, by replacing Eq. (3.8) into Eq. (3.12), we get

$$\sqrt{3}M^2\left[1 + \cos\left(\frac{\phi}{f}\right)\right]^{1/2}\dot{\phi} = \frac{M^4}{f}\sin\left(\frac{\phi}{f}\right), \tag{3.11}$$

and finally, solving for ϕ, we get the following result in the slow-roll approximation

$$\phi = f\arccos\left[2\tanh\left[\operatorname{arctanh}\left(\frac{\sqrt{\cos(\phi_{ini}/f) + 1}}{\sqrt{2}}\right) - \frac{M^2}{\sqrt{6}f^2}t\right]^2 - 1\right]. \tag{3.12}$$

Then, by the definition of $H = \dot{a}/a$, Eq. (3.8) transforms into

$$\frac{\dot{a}}{a} = \frac{M^2}{\sqrt{3}}\left[1 + \cos\left(\frac{\phi}{f}\right)\right]^{1/2}, \tag{3.13}$$

so, using the solution for ϕ found in Eq. (3.12), we obtain the solution for the scale factor

$$a = \exp\left[-2f^2\left[\log\left(\cosh\left(\operatorname{arctanh}\left(\frac{\sqrt{\cos(\phi_{ini}/f) + 1}}{\sqrt{2}}\right) - \frac{M^2}{\sqrt{6}f^2}t\right)\right)\right.\right.$$
$$\left.\left. - \log\left(\cosh\left(\operatorname{arctanh}\left(\frac{\sqrt{\cos(\phi_{ini}/f) + 1}}{\sqrt{2}}\right)\right)\right)\right].$$
$$\tag{3.14}$$

Finally, we can calculate the power spectrum with the slow-roll approximation by using Eq. (2.72). Furthermore, the result shows that the approximated value of the power spectrum calculated with the slow-roll approximation matches almost exactly the real value as presented in Fig. 3.4 and Fig. 2.7 (green line).

Chapter 4

Conclusions & Outlook

In this Thesis, we have reproduced the Power Spectrum for the Natural Inflation model (NI) into the slow-roll approximation. We have shown that the slow-roll approximation is a powerful tool that helps to study the behavior of a model in a more simple way. Specifically for the Natural Inflation model, the slow-roll approximation makes an almost perfect match with the predictions of the pure Natural Inflation model solved with the complete Friedmann equations.

The results obtained from the scalar power spectrum shown in Fig. (3.4) and in Fig. (2.7) are similar, meaning that the solutions obtained from the slow-roll approximation match almost perfectly with the solutions of the complete Friedmann equations. Thus, showing just a variation of a few units in the same order, $P_S \sim 3.51 \times 10^{-9}$ for Planck Collaboration results and $P_S \sim 2.0 \times 10^{-9}$ for slow-roll approximation, at 2σ confidence level, with an energy scale of inflation of $\Lambda = (7.8 \pm +6935780.5) \times 10^{15}$ GeV [14][52]. Additionally, the behavior of the scale parameter $a(t)$ shown in Fig. (3.3), explains that inflation must be accelerated given that the scale parameter increases exponentially with time as $a(t) \propto e^{Ht}$.

The Natural Potential describes and makes appropriate predictions of the inflation model, and it explains how the Universe began, more specifically, the accelerated expansion of the Universe. This type of potential presents enough flatness by which it produces the necessary amount of inflation, so that it is possible to explain the homogeneity, and ensures the proper normalization for the anisotropies observed in the CMB.

We used Python in order to get a numerical solution for the inflaton scalar field (ϕ), the scale parameter ($a(t)$), and the power spectrum (P_s). Then, with the data obtained, we performed the

calculations and obtained the graphics for the observable P_s, the scale parameter $a(t)$, and also for the inflaton scalar field ϕ and the inflaton potential $V(\phi)$.

Further studies can be developed in order to have a better approach to the model, or in order to see the behavior of the observables when they are subjected to perturbations.

Bibliography

[1] others,, *et al.* Final results from the Hubble Space Telescope key project to measure the Hubble constant. *The Astrophysical Journal* **2001**, *553*, 47.

[2] Steigman, G. Primordial nucleosynthesis in the precision cosmology era. *Annu. Rev. Nucl. Part. Sci.* **2007**, *57*, 463–491.

[3] Fields, B. D.; Olive, K. A. Big bang nucleosynthesis. *Nuclear Physics A* **2006**, *777*, 208–225.

[4] Iocco, F.; Mangano, G.; Miele, G.; Pisanti, O.; Serpico, P. D. Primordial Nucleosynthesis: from precision cosmology to fundamental physics. *Physics Reports* **2009**, *472*, 1–76.

[5] Fixsen, D.; Cheng, E.; Gales, J.; Mather, J. C.; Shafer, R.; Wright, E. The cosmic microwave background spectrum from the full cobe* firas data set. *The Astrophysical Journal* **1996**, *473*, 576.

[6] Dodelson, S.; Schmidt, F. *Modern cosmology*; Academic press, 2020.

[7] Kappl, R.; Nilles, H. P.; Winkler, M. W. Modulated natural inflation. *Physics Letters B* **2016**, *753*, 653–659.

[8] Hoefer, C. Einstein's struggle for a Machian gravitation theory. *Studies in History and Philosophy of Science Part A* **1994**, *25*, 287–335.

[9] Albrecht, A.; Steinhardt, P. J. Cosmology for grand unified theories with radiatively induced symmetry breaking. *Physical Review Letters* **1982**, *48*, 1220.

[10] Bardeen, J. M.; Steinhardt, P. J.; Turner, M. S. Spontaneous creation of almost scale-free density perturbations in an inflationary universe. *Physical Review D* **1983**, *28*, 679.

[11] Adams, F. C.; Bond, J. R.; Freese, K.; Frieman, J. A.; Olinto, A. V. Natural inflation: Particle physics models, power-law spectra for large-scale structure, and constraints from the Cosmic Background Explorer. *Physical Review D* **1993**, *47*, 426.

[12] Freese, K.; Frieman, J. A.; Olinto, A. V. Natural inflation with pseudo Nambu-Goldstone bosons. *Physical Review Letters* **1990**, *65*, 3233.

[13] Kachru, S.; Kallosh, R.; Linde, A.; Maldacena, J.; McAllister, L.; Trivedi, S. P. Towards inflation in string theory. *Journal of Cosmology and Astroparticle Physics* **2003**, *2003*, 013.

[14] others,, *et al.* Planck 2018 results. VI. Cosmological parameters. **2020**,

[15] Smoot, G. F. COBE observations and results. 1999.

[16] Liddle, A. R.; Lyth, D. H. *Cosmological inflation and large-scale structure*; Cambridge university press, 2000.

[17] Liddle, A. *An introduction to modern cosmology*; John Wiley & Sons, 2015.

[18] Alpher, R. A.; Herman, R. *Genesis of the big bang*; Oxford University Press, 2001.

[19] Smith, Q. The uncaused beginning of the universe. *Philosophy of Science* **1988**, *55*, 39–57.

[20] Frieman, J. A.; Turner, M. S.; Huterer, D. Dark energy and the accelerating universe. *Annu. Rev. Astron. Astrophys.* **2008**, *46*, 385–432.

[21] Afshordi, N.; Loh, Y.-S.; Strauss, M. A. Cross-correlation of the cosmic microwave background with the 2MASS galaxy survey: Signatures of dark energy, hot gas, and point sources. *Physical review D* **2004**, *69*, 083524.

[22] Henry, J. P. A measurement of the density parameter derived from the evolution of cluster X-ray temperatures. *The Astrophysical Journal* **1997**, *489*, L1.

[23] Peebles, P. J. E. Discovery of the hot Big Bang: What happened in 1948. *The European Physical Journal H* **2014**, *39*, 205–223.

[24] Friedman, A. Über die krümmung des raumes. *Zeitschrift für Physik* **1922**, *10*, 377–386.

[25] Lemaître, G. Un Univers homogène de masse constante et de rayon croissant rendant compte de la vitesse radiale des nébuleuses extra-galactiques. *Annales de la Société Scientifique de Bruxelles, A47, p. 49-59* **1927**, *47*, 49–59.

[26] Hubble, E. A relation between distance and radial velocity among extra-galactic nebulae. *Proceedings of the national academy of sciences* **1929**, *15*, 168–173.

[27] Riess, A. G.; Macri, L.; Casertano, S.; Lampeitl, H.; Ferguson, H. C.; Filippenko, A. V.; Jha, S. W.; Li, W.; Chornock, R. A 3% solution: determination of the Hubble constant with the Hubble Space Telescope and Wide Field Camera 3. *The Astrophysical Journal* **2011**, *730*, 119.

[28] others,, *et al.* A 2.4% determination of the local value of the Hubble constant. *The Astrophysical Journal* **2016**, *826*, 56.

[29] Hamuy, M.; Phillips, M.; Maza, J.; Suntzeff, N. B.; Schommer, R.; Aviles, R. A Hubble diagram of distant type IA supernovae. *The Astronomical Journal* **1995**, *109*, 1–13.

[30] others,, *et al.* Planck 2015 results-xiii. cosmological parameters. *Astronomy & Astrophysics* **2016**, *594*, A13.

[31] Reid, M.; Braatz, J.; Condon, J.; Lo, K.; Kuo, C.; Impellizzeri, C.; Henkel, C. The megamaser cosmology project. IV. A direct measurement of the Hubble constant from UGC 3789. *The Astrophysical Journal* **2013**, *767*, 154.

[32] Gao, F.; Braatz, J.; Reid, M.; Lo, K.; Condon, J.; Henkel, C.; Kuo, C.; Impellizzeri, C.; Pesce, D.; Zhao, W. The megamaser cosmology project. VIII. A geometric distance to NGC 5765b. *The Astrophysical Journal* **2016**, *817*, 128.

[33] others,, *et al.* H0LiCOW–IV. Lens mass model of HE 0435- 1223 and blind measurement of its time-delay distance for cosmology. *Monthly Notices of the Royal Astronomical Society* **2017**, *465*, 4895–4913.

[34] others,, *et al.* A gravitational-wave measurement of the Hubble constant following the second observing run of Advanced LIGO and Virgo. *The Astrophysical Journal* **2021**, *909*, 218.

[35] Branch, D. Type Ia supernovae and the Hubble constant. *Annual Review of Astronomy and Astrophysics* **1998**, *36*, 17–55.

[36] Pitrou, C.; Coc, A.; Uzan, J.-P.; Vangioni, E. Precision big bang nucleosynthesis with improved Helium-4 predictions. *Physics Reports* **2018**, *754*, 1–66.

[37] Boesgaard, A. M.; Steigman, G. Big Bang nucleosynthesis: theories and observations. *Annual Review of Astronomy and Astrophysics* **1985**, *23*, 319–378.

[38] Gawiser, E.; Silk, J. The cosmic microwave background radiation. *Physics Reports* **2000**, *333*, 245–267.

[39] Wright, E. L. Theoretical overview of cosmic microwave background anisotropy. *arXiv preprint astro-ph/0305591* **2003**,

[40] others,, *et al.* Seven-year wilkinson microwave anisotropy probe (WMAP*) observations: Are there cosmic microwave background anomalies? *The Astrophysical journal supplement series* **2011**, *192*, 17.

[41] Helbig, P. The flatness problem and the age of the Universe. *Monthly Notices of the Royal Astronomical Society* **2020**, *495*, 3571–3575.

[42] Senatore, L. Lectures on inflation. *Theoretical Advanced Study Institute in Elementary Particle Physics: new frontiers in fields and strings* **2016**, 447–543.

[43] Clesse, S. An introduction to inflation after Planck: from theory to observations. *arXiv preprint arXiv:1501.00460* **2015**,

[44] Polchinski, J.; Vieira, P.; Dewolfe, O. *New Frontiers in Fields and Strings (TASI 2015)-Proceedings of the 2015 Theoretical Advanced Study Institute in Elementary Particle Physics*; World Scientific, 2016.

[45] Goldhaber, G. The acceleration of the expansion of the universe: a brief early history of the Supernova Cosmology Project (SCP). 2009.

[46] Filippenko, A. V.; Riess, A. G. Results from the high-z supernova search team. *Physics Reports* **1998**, *307*, 31–44.

[47] Agarwal, N.; Bean, R. Cosmological constraints on general, single field inflation. *Physical Review D* **2009**, *79*, 023503.

[48] Zarei, M. On the running of the spectral index to all orders: a new model-dependent approach to constrain inflationary models. *Classical and Quantum Gravity* **2016**, *33*, 115008.

[49] Noble, C. D.; Herzog, J. M.; Rothamer, D. A.; Ames, A. M.; Oakley, J.; Bonazza, R. Scalar power spectra and scalar structure function evolution in the Richtmyer–Meshkov instability upon reshock. *Journal of Fluids Engineering* **2020**, *142*.

[50] Ruehle, F.; Wieck, C. Natural inflation and moduli stabilization in heterotic orbifolds. *Journal of High Energy Physics* **2015**, *2015*, 1–19.

[51] Barrie, N. D.; Kobakhidze, A.; Liang, S. Natural inflation with hidden scale invariance. *Physics Letters B* **2016**, *756*, 390–393.

[52] Linde, A. *Inflationary cosmology after Planck*; Oxford University Press Oxford, England, UK, 2015; Vol. 100.